Indian Journal of Pure & Applied Physics
Vol. 64, March 2026, pp. 283-291
DOI: 10.56042/ijpap.v64i3.25368

A Modified SRR Patch Antenna for Multiband Wireless Applications

Allin Joe D[a*] & Thiyagarajan K[b]

[a]Department of Electronics and Communication Engineering, Kumaraguru College of Technology, Coimbatore, 641 035, India
[b]Department of Electronics and Communication Engineering, PSG College of Technology, Coimbatore, 641 004, India

Received: 7th November 2025; accepted: 19th January 2026

Split Ring Resonator (SRR) antennas provide better electromagnetic characteristics and are used in various wireless applications. The designed antenna is developed on a cost effective FR4 substrate with dimensions of 35 x 35 mm² that features a simple and effective radiating geometry over it. This paper provides an overview of SRR antennas, with a focus on their design, mechanism, and ability to use in multiple frequency bands. The novelty of the designed SRR antennas is in their ability for manipulating the electromagnetic wave in the presence of resonators for the desired applications. The SRR antenna, with a focus on the use of slots in ground planes is used for improvement in frequency and bandwidth in wireless communication systems. Partial ground planes are used in the designed antenna for further improvement of radiation characteristics. The designed antenna is fabricated and measured for the validation of results. The measured results confirm that the designed antenna shall be utilized in worldwide interoperability for microwave access (WiMAX) communication, industrial, scientific, and medical radio band (ISM) communication, and in Sub-7 GHz fifth generation (5G) wireless communication.

Keywords: FR4, Multiband antenna, Patch resonator, Radiation pattern, Slots, SRR

1 Introduction

Resonator patch antennas consist of a conducting radiating element fabricated on a dielectric substrate for the transmission and reception of electromagnetic radiation. Their frequency of operation and radiation characteristics are determined by the physical dimensions and geometry of the patch. One of the most common forms is the microstrip patch antenna, which consists of a radiating patch on one side of a substrate and a ground plane on the other side. Patch antennas can be considered as compact and lightweight antennas, and they can be designed to operate at desired frequency and polarization. Patch antenna designs are limited by a narrow bandwidth and large electrical size at lower microwave frequencies. The integration of metamaterial inspired structures like SRR into the patch antenna is used to reduce these limitations[1].

The adoption of SRR in antenna design requires a knowledge of metamaterials to improve performance parameters. Metamaterials represent artificially created composite media that exhibit electromagnetic characteristics that are not found naturally. SRR structure consist of concentric rings of a conducting material interrupted by a split. This formulation operates as a resonating magnetic dipole that create an area of negative permeability close to their resonating frequency[2].

The ability to perform antenna miniaturization, bandwidth improvement, as well as implementing multiband performance from a single radiating source is possible by integration of SRR structures into patch antennas. The performance of SRR antenna is controlled by electromagnetic coupling between the patch and SRR structures. The integration of SRR structures into patch antenna designs, be it in the substrate or close to the feeding mechanism, allows the control of antenna performance characteristics[3]. Common approaches include placing SRR arrays in the antenna substrate or adjacent to the feed line. While this is effective, these methods will increase design complexity[4].

The requirement for miniaturized wireless devices that support multiple communications standards has led to intense investigations on the development of multiband antennas. WiMAX standard is used for closing the digital divide for rural and distant areas. It has wide area coverage and offers faster data rates[5]. Communications in the ISM bands such as Wi-Fi, Bluetooth, Zigbee, and LoRa provides economical communications. The unlicensed use of the ISM bands has led to an innovation by making them the

*Corresponding author: E-mail: allinjoe.d.ece@kct.ac.in

foundation for modern local area networks and the internet of things (IoT) environment. The sub-7 GHz 5G system provides reliability and low latency. It shall be used in the emerging technologies like autonomous systems[6]. The convergence of the above three technologies offers a single smart system with the combined strengths of each technology. It also provides flexibility and connectivity to manage the requirements in smart infrastructures and next generation broadbands[7].

This paper presents the design and experimental validation of a compact triple band antenna for modern wireless applications. In this work, a modified SRR geometry is integrated in the patch antenna for multiband operation. The design approach focuses on the SRR geometrical inclusions within the resonating patch for better performance of designed antenna. This integration perturbs the patch antennas fundamental and higher order modes more effectively than externally placed SRR. This introduces additional resonant frequencies and improves impedance matching[8]. Optimization of the antenna performance is achieved by incorporating slots in the ground plane along with partial ground plane structure. Partial ground plane provides more current paths for providing a stable radiation. These combined modifications will alter the surface current paths as well as impedance characteristics and excite multiple resonant modes of antenna[9]. The design parameters involve the SRR dimensions like ring radius, gap width, and split orientation. Patch geometry, ground plane slot configuration, and the size of the partial ground plane also has a major role in antenna radiation characteristics[10]. The uniqueness of the proposed design is that the designed antenna utilizes the electromagnetic coupling between the patch, the split ring resonators, and the truncated ground for achieving desired performance instead of loading the metamaterials.

In a microstrip patch antenna, the choice of substrate affects both electrical and magnetic properties. The relative permittivity of the substrate, thickness of the substrate and loss tangent of the substrate influence the radiation characteristics of microstrip patch antenna. FR4 is one of the most employed substrate materials in antenna designs. FR4 has a high dielectric constant, allowing the physical dimension of the patch antenna to be reduced for a particular resonant frequency. FR4 is compatible with partial ground topologies because of its relatively high dielectric constant[11]. The partial ground plane increases the fringing fields, and the use of FR4 is beneficial for the electromagnetic coupling between the patch and the ground plane. It also exhibits high mechanical and thermal stabilities. The major advantage of using the FR4 substrate is the low cost associated with it compared to other microwave materials[12].

Rogers RO4000, Taconic RF-35 and RT/duroid materials are used in high frequency antenna designs. The advantage of these materials includes a low and stable dielectric value accompanied by a low loss tangent value that represents low signal dissipation and low moisture absorption. The cost of these materials is much higher than FR4[13]. Ceramic material like Alumina has a high dielectric constant (ε_r) and a very low loss tangent. The high ε_r helps create antenna designs significantly smaller in size as the patch antenna's dimension is inversely proportional to the square root of ε_r. It shall be used in small IoT modules. Its disadvantages are brittle nature and limited bandwidth[14]. Flexible material like Polyimide is moderately good in terms of electrical characteristics and possess a relatively lower value of the loss tangent. The drawback is that, depending upon the bending, the effective dielectric constant will vary[15]. FR4 substrate material is significant in making the proposed patch antenna design efficient since it is rugged and inexpensive.

The proposed antenna is implemented on an FR4 substrate without requiring stacked layers and complicated feeding networks. The design differs from other reported SRR based antennas, as they mostly employ costly substrates or stacked designs[16]. The designed antenna presents an improved impedance bandwidth without increasing the antenna size, which is difficult for patch antennas loaded with SRRs[17]. The proposed antenna offers a good multiband performance with the aid of a low cost FR4 substrate and compact size. Adding the concept of the partial ground plane, along with the strategically placed SRR, improves the bandwidth characteristics of the proposed antenna.

The designed antenna is fabricated on a FR4 dielectric substrate. Experimental verification was made based on the Vector networl analyzer (VNA) measurements to analyze the scattering parameters, where the reflection coefficient (S_{11}) is estimated. The radiation patterns are measured in the anechoic chamber. A comparative study of the simulated models against the experimental results is carried out to validate the principles behind the design and

demonstrate the performance improvements brought by the modified SRR and slotted ground plane configuration. This paper concludes with a discussion of the obtained multiband performance metrics through the proposed modifications.

2 Materials and Methods

2.1 Multiband Antenna Design

The process of designing the multiband antenna begins with the design of the patch antenna using High Frequency Structure Simulator (HFSS) software. Multiband capabilities are achieved in the patch antenna by incorporating resonator patches into the design of the patch antenna. Improvements in impedance matching are achieved by the addition of slots on the ground plane of the antenna. Further improvement in performance is achieved by using partial ground planes. Addition of the slots in the ground plane of the antenna, as well as the partial ground plane structures contributes to the miniaturization of the antenna design.

A SRR may be analyzed using a miniature LC resonant circuit, wherein the ring portion is the inductive element, while the gap portion is the capacitive element. As the SRR increases in size, the inductive effect enhances, and the resonant frequency reduces. On the contrary, as the SRR reduces in size, the resonant frequency rises. Based on the chosen SRR configuration, the resonant frequency can be adjusted to match the desired operating frequency of the antenna. A smaller SRR gap enhances capacitance and decreases the resonant frequency. A larger gap reduces coupling between the antenna elements. A suitable gap width is chosen to ensure impedance matching. SRRs are placed in areas of high current flow or high electric fields within the patches[18].

2.1.1 Modified SRR

The SRR geometry shown in Fig. 1 has two concentric split rings. This induces a vertical magnetic field. This vertical magnetic field utilizes negative permittivity values. The side length of inner ring is represented as l_1 and the outer ring side length is represented as l_2. The split gap between the inner ring and outer ring is denoted by g_1 and g_2. The gap between the inner and outer rings is represented by g_3. The split gap as well as the gap between the rings generates capacitance, aiding in the control of the structure's resonance. When subjected to an oscillating electromagnetic field, SRR exhibit an electrical size reduction effect. To utilize the advantages of the SRR in the designed antenna, the structure of SRR shall be modified and utilized based on the desired applications[19].

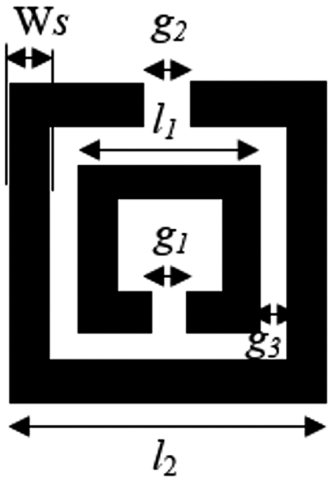

Fig. 1 — Geometry of SRR

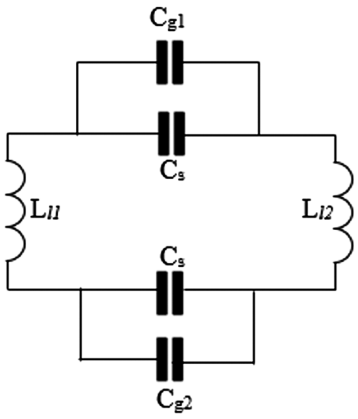

Fig. 2 — Equivalent circuit of SRR

The modified SRR structure will enable the patch antenna to resonate at multiple frequencies and will meet the evolving needs of modern tele-communications. SRR shall be modeled as an electrical equivalent circuit as shown in Fig. 2. The aperture opening in the rings l_1 and l_2 denoted as g_1 and g_2 are designed as capacitors C_{l1} and C_{l2} in the equivalent circuit. Additionally, capacitance also arises between the rings due to the gaps present between the SRR rings and are designated as C_s. The rings of SRR are made of a conductor and will interact through the capacitor C_s which creates the inductance in the SRR rings denoted as L_{l1} and L_{l2}.

SRR structure has the characteristic of an LC equivalent circuit. The equivalent inductance L_l of L_{l1} and L_{l2} are obtained by[20],

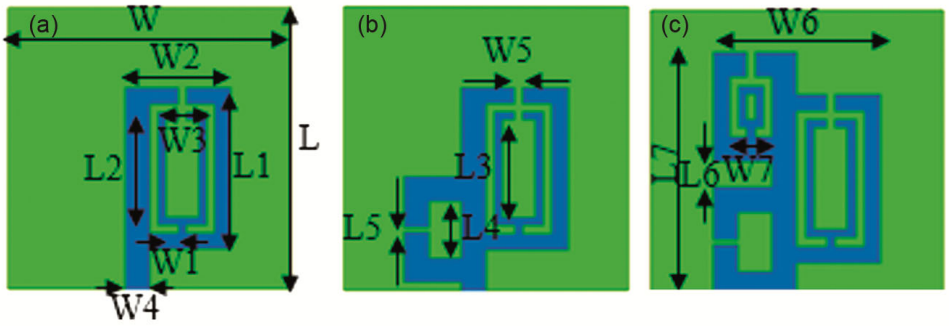

Fig. 3 — Evolution of patch resonator

$$L_l = L_{l1} = L_{l2} = \frac{\mu_0 g_3}{W_s} [l_1 + l_2] \quad \ldots (1)$$

Consider A_{s1} and A_{s2} are the area of the inner ring and outer ring of the SRR structure and let W_s be the width of the SRR structure. The capacitance that arises due to the split gaps g_1 and g_2 are C_{g1} and C_{g2} and are obtained by,

$$C_{g1} = \frac{\varepsilon_0 \varepsilon_r A_{s1}}{g_1} \quad \ldots (2)$$

$$C_{g2} = \frac{\varepsilon_0 \varepsilon_r A_{s2}}{g_2} \quad \ldots (3)$$

The value of μ_0 is 1.256 x 10^{-6} N/A^2 and the value of ε_0 is 8.854 x 10^{-12} F/m. The value of C_s is given by,

$$C_s = \frac{A\varepsilon_0\varepsilon_r W_s [2l_2 + 2l_1 - g_1]}{g_3} \quad \ldots (4)$$

where A is equilibrium constant. Consider the gap capacitance of the split gaps g_1 and g_2 are equal and let C_g be the corresponding capacitance then the resonant frequency (f_r) generated by the SRR structure is given by,

$$f_r = \frac{1}{2\pi \sqrt{L_l [C_g + C_s]}} \quad \ldots (5)$$

2.1.2 Patch Resonator

A square FR4 substrate with 35 mm x 35 mm x 1.6 mm dimension is chosen for the antenna design. Over this substrate, a resonator patch is placed. The antenna design is implemented in HFSS software. HFSS can simulate electromagnetic fields, surface currents, and scattering parameters within a given frequency range. Return loss is the amount of power reflected to the source due to impedance mismatch between the antenna and the transmission line. The return loss in HFSS can be determined by exciting the antenna through a port and measuring the reflected energy at the same port. With precise input of geometry, material, ports, boundary conditions, and

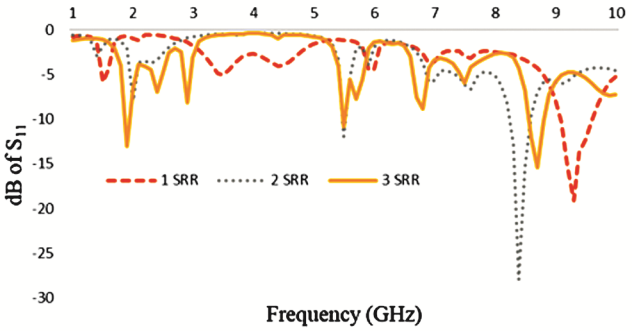

Fig. 4 — Return loss of the patch resonator shapes

frequency range, return losses in an antenna can be determined. In HFSS simulation, return loss is derived from S parameter analysis as S_{11}.

The evolution of the patch resonator is shown in Fig. 3. The length components of the patch resonator are given as: L = 35 mm, L1 = 20 mm, L2 = 14 mm, L3 = 13 mm, L4 = 7 mm, L5 = 0.8 mm, L6 = 3 mm and L7 = 29 mm. The width components of the patch resonator are given as: W = 35 mm, W1 = 1 mm, W2 = 10 mm, W3 = 5 mm, W4 = 3 mm, W5 = 1 mm, W6 = 19 mm and W7 = 5 mm. The return loss of the designed patch resonator shapes is plotted in Fig. 4. The designed antenna utilizes a microstrip feed mechanism to excite its resonator structure. Initially, a single SRR structure is created in patch as shown in Fig. 3 (a) that has a resonant frequency of 9.3 GHz with a return loss of 19.05 dB and bandwidth as 529 MHz. To introduce additional resonant frequencies in the antenna structure, two SRR structures are created as shown in Fig. 3 (b) and it resonates at two frequencies. The resonant frequencies are 5.5 GHz and 8.4 GHz, with return loss values as 11.94 dB and 27.91 dB, respectively. The generated bandwidths for these resonant frequencies are 35 MHz and 341 MHz, respectively. By introducing the additional SRR structure, the fundamental resonant frequency is shifted to a lower frequency.

The bandwidth of the two SRR structures is much lesser than the one SRR antenna structure. To improve beyond, a third SRR structure as shown in Fig. 3 (c) is created which generates three resonant frequencies at 1.9 GHz, 5.5 GHz, and 8.9 GHz. The fundamental resonant frequency generated by the three SRR antenna structure is significantly lower compared to that of the one and two SRR antenna configurations. The fundamental resonance occurs at 1.9 GHz, with a return loss of 13.04 dB and a narrow bandwidth of 69 MHz. Subsequently, the next order of resonance is observed at 5.5 GHz with a return loss of 10.81 dB and a much narrower bandwidth of 17 MHz. Finally, the higher order resonance occurs at 8.7 GHz, displaying a return loss of 15.44 dB and a bandwidth of 204 MHz. Overall, the three SRR antenna structure exhibits superior multiband and bandwidth characteristics compared to the other SRR antenna configurations. The combined inductance value of the three SRR structure is L_{SRR} and its combined capacitance value is C_{SRR}, then the resonant frequency of the three SRR patch resonator structure (f_{SRR}) is,

$$f_{SRR} = \frac{1}{2\pi \sqrt{L_{SRR}\, C_{SRR}}} \quad \ldots (6)$$

The generated return loss values require improvement across all three resonant frequencies. Introducing slots in the ground of the patch resonator antenna structure can improve return loss values at the generated resonant frequencies.

2.1.3 Slots in Ground Plane of Patch Resonator

When a slot is introduced in the ground plane of patch antenna, it elongates the length of excited surface current. This, in turn, reduces the antenna's fundamental resonant frequency. As a result of this, the antenna's size becomes smaller compared to a conventional microstrip antenna operating at the same frequency[21]. When a slot is etched in ground plane, an additional series capacitance (C_{slot}) is generated due to the separation of the conducting planes by a gap filled with air. A series inductive effect (L_{slot}) is also generated across the length of the etched slot. Consequently, this etching of slot introduces series capacitance and series inductance to the equivalent circuit. The resultant inductance and capacitance values after introducing slot in the three SRR patch resonator is given by L_{eq} and C_{eq}. The resonant frequency (f_{eq}) of the designed three SRR patch resonator structure with the introduced slot is then determined by these additional elements[22].

$$f_{eq} = \frac{1}{2\pi \sqrt{L_{eq}\, C_{eq}}} \quad \ldots (7)$$

$$L_{eq} = L_{SRR} + L_{slot} \quad \ldots (8)$$

$$C_{eq} = \frac{C_{SRR}\, C_{slot}}{C_{SRR} + C_{slot}} \quad \ldots (9)$$

Larger slots result in a larger inductive path distance; hence the resonances shift to lower frequencies. Smaller slots decrease the inductive patch distance and shift the resonances to higher frequencies. In that manner, the chosen slot sizes have the best possible trade off concerning the bandwidth. On the capacitive side, smaller slots add greater amounts of capacitances due to their ability to confine the electric fields tightly, while larger slots add smaller amounts of capacitances[23].

For performance enhancement of the multiband three SRR patch resonator antenna structure, a single slot is created in ground as shown in Fig. 5 (a). It resonates at three distinct frequencies 1.9 GHz, 6.8 GHz, and 9.9 GHz, exhibiting return loss values of 12.7 dB, 15.6 dB, and 15.49 dB, respectively. The corresponding bandwidths generated are 108 MHz, 124 MHz, and 186 MHz. A second slot is formed below the first slot and is longer than the length of the first slot as shown in Fig. 5 (b). The designed antenna structure with two slots in ground resonates at 1.9 GHz, 5.5 GHz, and 6.9 GHz with return loss values as 16.41 dB, 12.46 dB and 20.51 dB. The generated bandwidths are 144 MHz, 51 MHz, and 193 MHz. A third slot is formed in ground located below the second slot which was longer than the previous slots as illustrated in Fig. 5 (c). The three slot antenna structure resonates at frequencies of 1.9 GHz, 6.7 GHz, and 8.6 GHz, with return loss values of 21.9 dB, 13.16 dB, and 18.24 dB, respectively. The resulting bandwidths are 187 MHz, 57 MHz, and 326 MHz. A fourth slot is made below the third slot, and its length is longer than all the previous slots as shown in Fig. 5 (d). The four slot antenna structure resonates at frequencies 5.3 GHz, 6.1 GHz, and 8 GHz, exhibiting return loss values of 13.81 dB, 11.77 dB, and 21.86 dB, respectively. The resulting bandwidths are 64 MHz, 31 MHz, and 315 MHz.

Figure 6 illustrates the influence of different slots in the ground plane of the three SRR patch resonator antenna. The fundamental frequency is 1.9 GHz for the first, second and third slot antenna structures. The lower fundamental frequency ceases while introducing the fourth slot and is shifted to a higher

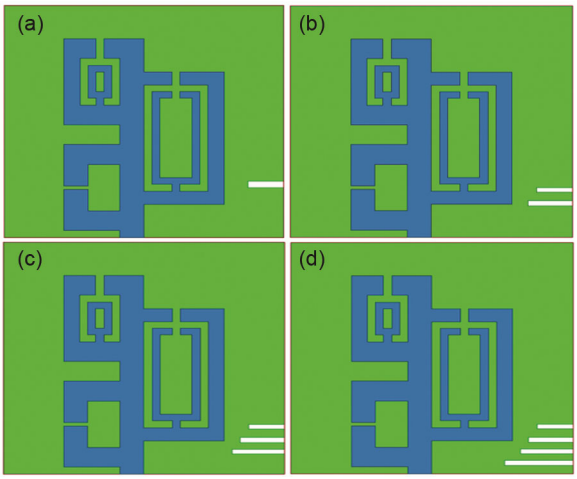

Fig. 5 — Slots in ground plane of patch resonator

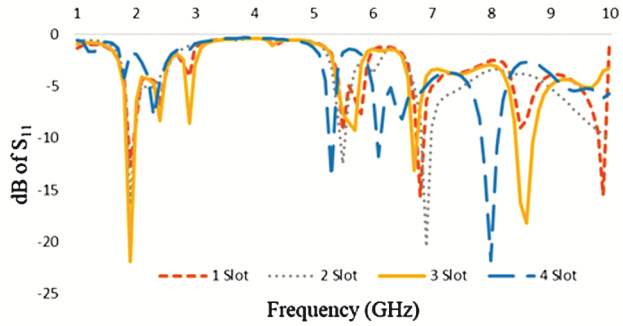

Fig. 6 — Return loss performance of slots in ground plane of patch resonator

5.3 GHz frequency. Maximum return loss values and the maximum bandwidth at the resonant frequencies are obtained at three slot antenna structure. Hence, this three slot antenna structure is chosen for further optimization. Partial ground structures shall be utilized for further enhancement of return loss and bandwidth characteristics of the chosen antenna.

2.1.4 Proposed Antenna

Reducing the length of the ground plane affects the electromagnetic boundary underneath the patch. This reduction allows the fringing fields to protrude outside the boundary of the patch. When partial ground structure is deployed in a patch antenna the inductance and capacitance values of the antenna will be modified. These alterations impact the resonant frequency, and impedance characteristics of the antenna. Introducing a partial ground structure effectively shortens the electrical length of the antenna, leading to a reduction in its inductance. This alteration can significantly impact both the resonant frequency and bandwidth of the designed antenna. Consequently, this modification reduces the inductive

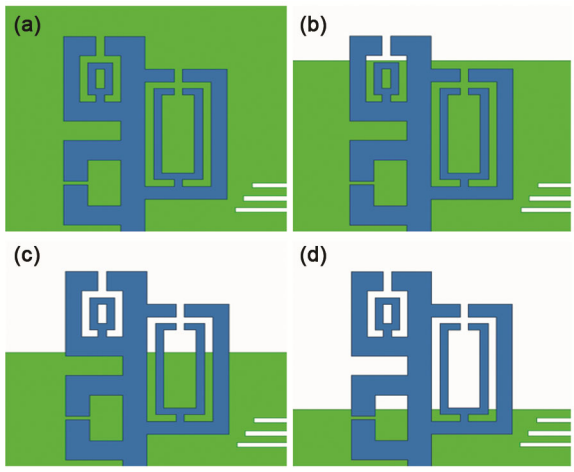

Fig. 7 — Partial ground planes in patch resonator with three slots in ground plane

reactance of the antenna. The partial ground structure introduces changes in the distribution of electric fields around the antenna. This alteration in field distribution leads to variations in capacitance. The inclusion of the partial ground structure increases the capacitance between the patch and the ground plane which in turn alters the antenna's impedance matching and radiation characteristics[24].

The ground plane is designed using parametric analysis for the purpose of obtaining a stable radiation pattern and canceling the higher order modes. Too much reduction in the ground plane results in the instability of the impedance levels. The full ground plane antenna structure (L) with 35 mm as dimension shall be reduced to three fourth (0.75L) of its length as 26.25 mm. Then it shall be decreased to half size (0.5L) as 17.5 mm in length and further reduced to quarter size (0.25L) as 8.75 mm. The different partial ground plane structures are analyzed for obtaining the optimal performance of the designed antenna. Figure 7 illustrates the various partial ground planes utilized in this work. The full ground plane structure in patch resonator with three slots in ground plane is illustrated in Fig. 7 (a). Figure 8 shows the return loss of the different partial ground planes in the designed patch resonator antenna. Antenna structure with a 0.75L partial ground plane, as shown in Fig. 7 (b), demonstrates resonance at frequencies of 1.9 GHz, 6.8 GHz, and 8.9 GHz, yielding return loss values of 15.06 dB, 16.65 dB, and 20.9 dB, respectively. These resonances result in bandwidths of 169 MHz, 153 MHz, and 301 MHz, respectively. Conversely, the 0.5L partial ground plane as illustrated in Fig. 7 (c) resonates at 2.8 GHz, 5.7 GHz, and 6.9 GHz, with

return loss values of 13.63 dB, 22.78 dB, and 17.08 dB. The bandwidths generated are 371 MHz, 202 MHz, and 197 MHz. Although this structure attains maximum bandwidth, the return loss at the first resonant frequency is less. When the ground plane is further reduced to 0.25L as shown in Fig. 7 (d), 2.8 GHz, 5.7 GHz, and 6.7 GHz resonant frequencies are generated with return loss values as 22.19 dB,

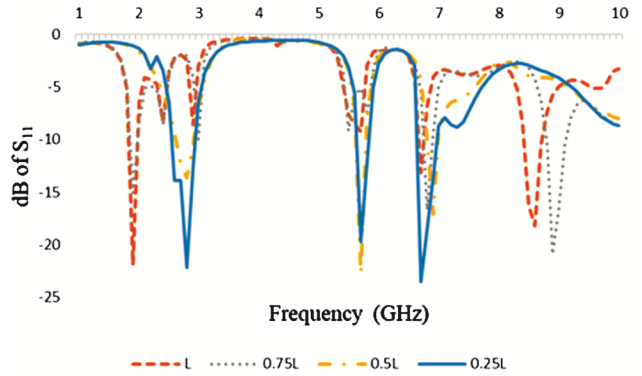

Fig. 8 — Return loss behaviour of partial ground planes in patch resonator with three slots in ground plane

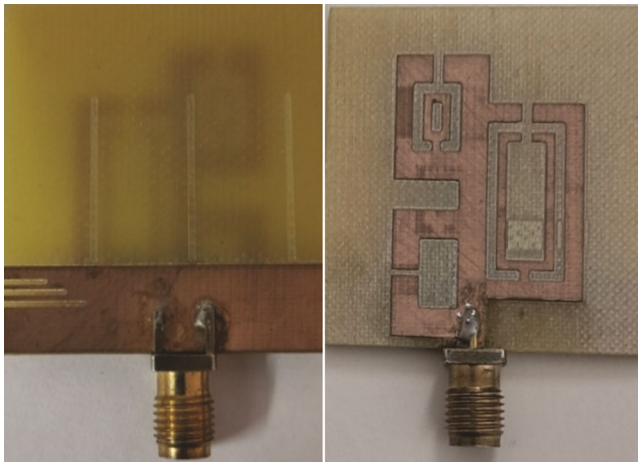

Fig. 9 — Top and bottom view of fabricated antenna

19.77 dB and 23.51 dB which is better than all other partial ground planes. The generated bandwidths are 335 MHz, 217 MHz, and 188 MHz. Hence, the 0.25L partial ground plane structure with three slots in the ground plane and three SRR structure in the patch is chosen as the proposed antenna.

3 Fabricated Antenna and Tested Results

Figure 9 displays both the top and bottom views of the fabricated antenna. Figure 10 shows the surface current distribution of the proposed SRR patch antenna at all its generated resonant frequencies. The currents flow along the patch defining the resonance of the fabricated antenna. The fundamental resonant frequency of 2.6 GHz is produced by the feed structure. The generated second resonant frequency of 5.7 GHz as well as the third resonant frequency of 7 GHz has its maximum effect from the initial modified SRR structure in the patch.

The return loss of the fabricated antenna, tested using a (VNA), is shown in Fig. 11. The tested results have three distinct resonant frequencies: 2.6 GHz, 5.7 GHz, and 7 GHz, with return loss values as 22.36 dB, 18.58 dB, and 19.45 dB, respectively. The first frequency band, ranging from 2.54 GHz to 2.75 GHz, aligns with the WiMAX wireless standard. 5.66 GHz to 5.87 GHz frequency range is the second frequency band which shall be utilized in the ISM wireless band. The third frequency band ranges from 7.06 GHz to 7.23 GHz, that shall be used in Sub-7 GHz 5G mobile applications. Figure 12 shows the comparison of simulated and tested return loss plots of the proposed antenna. The tested data of the proposed antenna aligns closely with the simulated data for the initial two resonant frequencies generated. The shift in the third resonant frequency between the simulated and

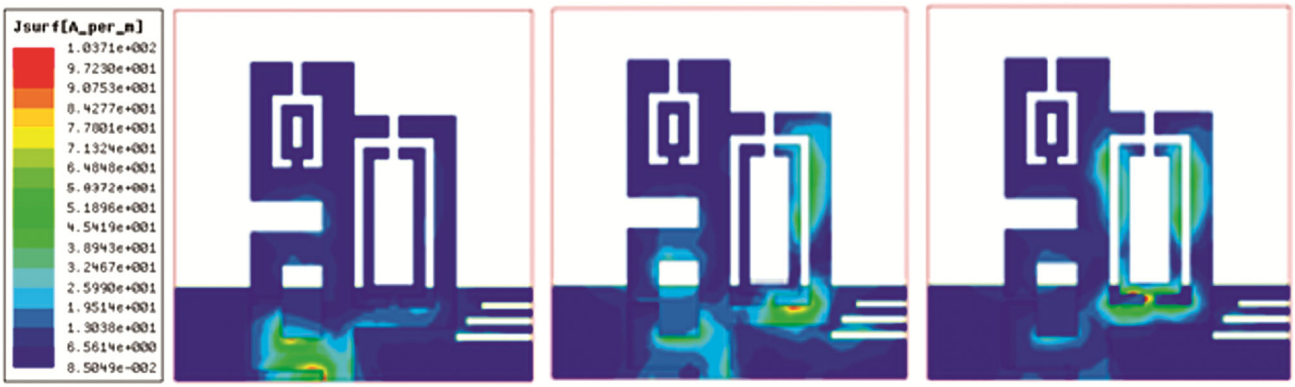

Fig. 10 — Electric field distribution of proposed antenna (a) 2.6 GHz (b) 5.7 GHz; and (c) 7 GHz

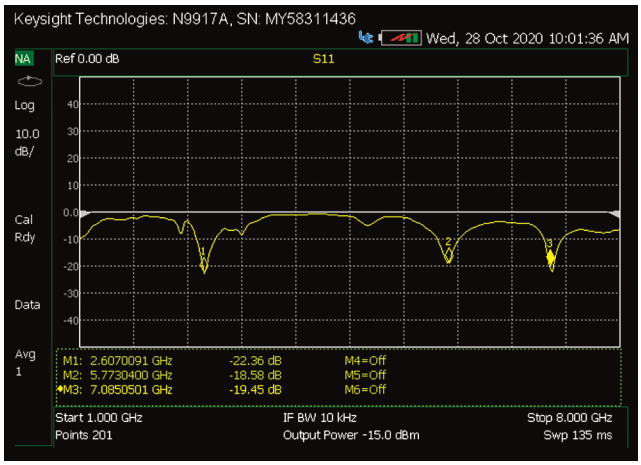

Fig. 11 — Tested return loss plot of fabricated antenna

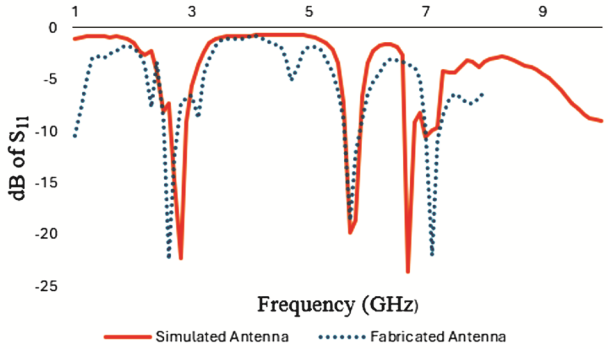

Fig. 12 — Simulated and tested return loss of proposed antenna

tested data is due to the irregularities in fabricating the closely aligned antenna structures.

The two-dimensional (2D) radiation pattern of a patch antenna illustrates how electromagnetic energy spreads in space. Patch antennas display a directional radiation pattern, with the highest radiation occurring in the broadside direction, perpendicular to the antenna surface. However, the pattern can differ based on factors such as antenna geometry, feed structure, and operating frequency. The fabricated antenna is tested using anechoic chamber for the radiation pattern characteristics and the results at each resonant frequencies are illustrated in Fig. 13. Measured results demonstrate good impedance matching across all operating frequency bands, confirming the antenna's suitability for compact wireless devices. A direct comparison of simulated and tested results is vital in the design of an antenna because it ensures the accuracy of the simulation results and the functionality of the developed physical antenna. As per the radiation pattern obtained from the tested

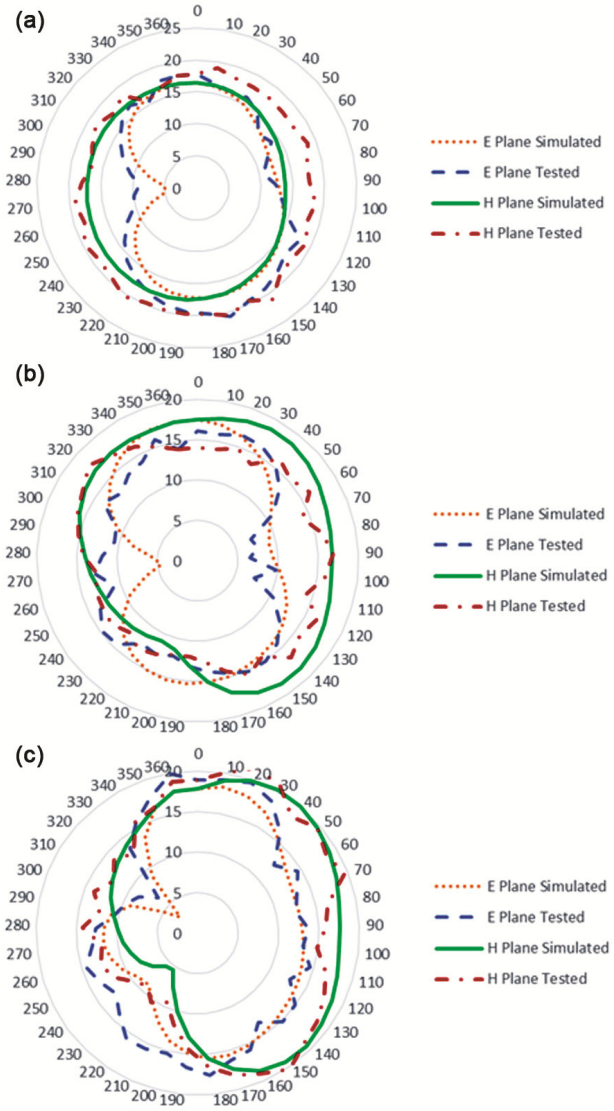

Fig. 13 — Simulated and tested 2D radiation plot of proposed antenna (a) 2.6 GHz (b) 5.7 GHz; and (c) 7 GH_Z

results, the fundamental resonant frequency of the fabricated antenna is 2.6 GHz. The E and H plane simulated and tested data of the fundamental resonant frequency are compared and is shown in Fig. 13 (a). The simulated and tested E plane and H plane radiation pattern for the obtained second resonant frequency of 5.7 GHz is shown in Fig. 13 (b). Figure 13 (c) shows the E plane and H plane 2D simulated and tested radiation patterns of the 7 GHz resonant frequency. A comparison of the tested results of the proposed antenna with the works available in the recent literature is presented in Table 1. This comparison validates the performance of the proposed antenna.

Table 1 — Comparison of proposed antenna with recent literature

Ref.	Method used	Size (mm^3)	Material and permittivity	Number of frequency band	Resonant frequencies (GHz)	Bandwidth (MHz)
[11]	Square SRR patch antenna	25 x 21.4 x 1.6	FR4, 4.4	1	5.85	430
[13]	SRR slots in patch, matching stubs	35 x 50 x 1.57	RT/ Duriod, 2.2	3	3, 4, 5	500
[17]	Electromagnetic band gap (EBG) structure, SRR antenna	98 x 109.4 x 3	wash cotton, 1.51	2	2.4, 5.4	374
This work	Three SRR patch, slots in partial ground plane antenna	35 x 35 x 1.6	FR4, 4.4	3	2.6, 5.7 & 7	590

4 Conclusion

The proposed SRR patch antenna resonator presents a promising solution for achieving multiband functionality in modern wireless communication systems. By leveraging the unique properties of split ring resonators, the narrow band limitation of the traditional patch antenna is eliminated. Introducing slots and partial ground planes in the designed antenna enhances its bandwidth across the resonant frequencies. The proposed antenna has wider frequency coverage and improved multiband operation. The proposed antenna is then fabricated and tested. The tested results validate the antenna for three wireless communication standards. The optimization algorithms shall be utilized in the future work to alter the dimensions and geometry of the modified SRR structure as well as patch. This will improve the radiation performance of the designed antenna. Moreover, this design can be expanded to a frequency reconfigurable antenna by adding active components, such as varactor diodes, across the gap of the SRR for the electronic tuning of the higher frequency bands.

References

1 Zhu L & Liu N, *Electromagnetic Sci*, 1 (1) (2023) 1.

2 Mukherjee B, Patel P & Mukherjee J, *J Electromagnetic Waves Appl*, 34 (2020) 1.

3 Iyer A K, Alu A & Epstein A, *IEEE Trans Antennas Propag*, 68 (3) (2020) 1223.

4 Sharma A K, Sharma V, Agarwal P, Nainwal A & Singh S, *Microwave Review*, 31 (2) (2025) 9.

5 Rajeshkumar V & Rajkumar R, *Progress Electromagnetics Res Lett*, 95 (2021) 43.

6 Kale S R & Patil D P, *Phys Scr*, 100 (9) (2025) 095532.

7 Allin Joe D & Thiyagarajan K, *Adv Electr Comp Eng*, 25 (3) (2025) 37.

8 Valipour A, Kargozarfard M H, Rakhshi M, Yaghootian A & Sedighi H M, *J Mater Des Appl*, 236 (11) (2022) 2171.

9 Tadesse A D, Acharya O P & Sahu S, *Int J RF Microw Comp-Aided Eng*, 30 (5) (2020) e22154.

10 Allin Joe D & Krishnan T, *Int J Antennas Propag*, 2023 (2023) 1.

11 Ajewole B D, Kumar P & Afullo T J, "Square SRR metamaterial inspired microstrip antenna for wireless mobile communication," in Proceedings of the International Conference on Artificial Intelligence, Big Data, Computing and Data Communication Systems, Durban, South Africa, 1–6 August 2021.

12 Vazquez F, Villareal A, Rodriguez A, Martin R, Solis Najera S & Rodriguez Melendez O R, "Electric field sensing with a modified SRR for wireless telecommunications dosimetry," Electronics, 10 (3) (2021) 295.

13 Mishra R, Dandotia R, Mishra R, Kuchhal P & Pachauri R, "SRR slotted multiband antenna in sub 6-GHz for futuristic communication," EAI Endorsed Transactions on Energy Web, 8 (32) (2018) 165997.

14 Wang B, Han B, Li Y, Gao F, Chen C, He J & Wang K, *Coatings*, 13 (7) (2023) 1213.

15 Prabhu S S & Tharini C, *Progress Electromagnetics Res C*, 153 (2025) 141.

16 Han Z, Kohno K, Fujita H, Hirakawa K & Toshiyoshi H, *IEEE J Selected Topics Quantum Electron*, 21 (4) (2015) 114.

17 Wajid A, Ahmad A, Ullah S, Choi D & Islam F, "Performance analysis of wearable dual-band patch antenna based on EBG and SRR surfaces," Sensors, 22 (14) (2022) 5208.

18 Omar A R S, Al-Hammami K A, Qwakneh M M & Faouri Y S, "Frequency reconfigurable antenna inspired by tri-SRR metamaterial," in Proceedings of the IEEE International Conference on Communication, Networks and Satellite (Comnetsat), (2020) 296–300.

19 Ucar M, *Appl Comp Electromagnetics Soc J*, 36 (6) (2021) 779.

20 Naoui S, Latrach L & Gharsallah A, Int J Microw Optical Technol, 11 (1) (2016) 1.

21 Majji N K, Madhavareddy V N, Immadi G, Ambati N & Aovuthu S M, EngTechnol Appl Sci Res, 14 (1) (2024) 12445.

22 Krishnan T, Sennan S, Ravi V & Reddy D H, "A dual-band circular patch antenna using hexagon-shaped slots," Int J Comm Syst, 35 (9) (2022) e5125.

23 Ansari J A, Dubey S K & Mishra A, *Microw Optical Technol Lett*, 51 (6) (2009) 1576.

24 Peram A, Reddy A S & Prasad M N G, *Wireless Personal Comm*, 106 (3) (2019) 1275.